Studies of Ultracold Hydrogen

Principal Investigators

Prof. Daniel Kleppner and Prof. Thomas J. Greytak

Project staff

Stephen C. Moss, David Landhuis, Dr. Lorenz Willmann, Jan Heemskerk, Lia Matos, Julia K. Steinberger, Kendra Vant, Mukund Vengalattore

Sponsors

National Science Foundation, Office of Naval Research

1 Introduction

Our group helped launch the search for atomic Bose-Einstein condensation (BEC) many years ago, working with spin-polarized hydrogen. BEC was discovered in experiments with alkali atoms in 1995 [1, 2, 3], and that discovery has revolutionized atomic physics. Three years later, we observed BEC with hydrogen. Hydrogen differs from the alkali metal atoms in many respects, and our cooling techniques, which are based on cryogenic cooling (as contrasted to laser cooling), are fundamentally different from those used in other experiments. Hence, in the world of BEC, atomic hydrogen occupies a unique position.

Recall that Bose-Einstein condensation is a pure quantum mechanical phase transition that takes place when the phase space density of a gas of bosons is approximately unity. More precisely, the condition for condensation is $n\Lambda_{th}^3 \geq 2.612$, where n is the density and $\Lambda_{th} = \sqrt{2\pi\hbar^2/mk_BT}$ is the thermal de Broglie wavelength. For H at a density of 4.8×10^{15} atoms$\cdot$cm^{-3}, the transition occurs at a temperature of ~ 65 μK. In an ideal gas, when condensation occurs a fraction of the atoms occupy the quantum ground state of the system, and the energy of an atom in this fraction is the zero point energy of the confining potential. In a real gas, however, interactions between the atoms elevate the condensate's energy. These interactions influence many of the properties of the condensate.

2 Description of experiment

Trapping There are major differences between H and the other Bose-condensed atoms: Li, Na, and Rb. Laser cooling and trapping methods are poorly suited to H. Consequently, we trap hydrogen using solely magnetic techniques [4], and we cool it through a combination of cryogenic techniques, magnetic "saddlepoint" evaporation, and rf evaporation. Our source of hydrogen is a cryogenic rf discharge operating at a temperature of 300 mK. Atoms emerging from the discharge are confined in a double-walled plastic cell of diameter 4 cm and length 60 cm. Thermal conductivity is provided by a 2 mm thick jacket of superfluid ^{4}He located between the two walls. The binding energy of hydrogen to the cell wall (an important parameter during the loading of the magnetic trap) is reduced to 1 K by covering the wall with a thin film of superfluid ^{4}He. To confine the atoms, superconducting coils in an "Ioffe-Pritchard" configuration produce a magnetic field with a minimum at the center of the cell. A maximum field of 0.9 T provides a magnetic trap depth of 0.5 K for atoms in the $F = 1$, $m_F = 1$ hyperfine state. By confining the atoms away from the cell wall, they can be cooled far below the cell temperature.

Evaporation After loading the magnetic trap, we cool the gas by forced evaporation. A saddlepoint in the magnetic field is slowly lowered. During collisions some atoms receive sufficient kinetic energy to escape from the trap. Their kinetic energy is greater than the average energy of the remaining atoms. As a result the temperature of the remaining atoms is reduced. In our trap the saddlepoint lies at the end of a long,

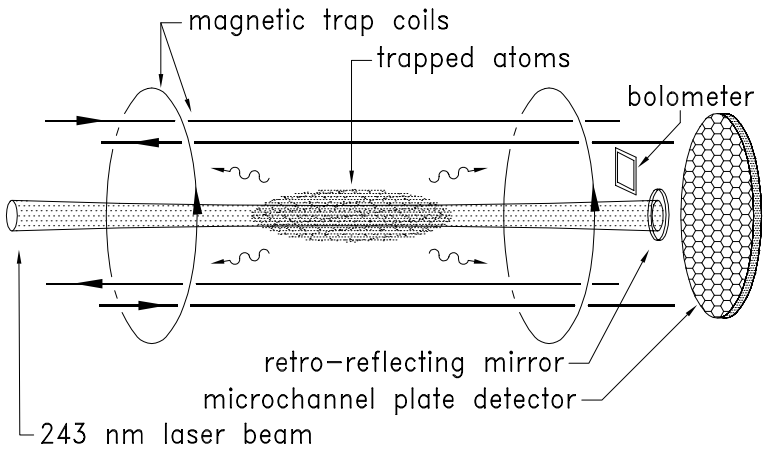

Figure 1: Schematic diagram of apparatus: Coils create a magnetic field with a minimum along the trap axis, which confines the sample. The 243 nm laser beam is focused to a 50 μm beam radius and retro reflected. Typically, a 1.5 ms laser pulse promotes some atoms to the metastable $2S$ state. An electric field then Stark-quenches the $2S$ atoms, and the resulting Lyman-α fluorescence photons are counted by the microchannel plate. Not shown is the trapping cell which surrounds the sample and is thermally anchored to a dilution refrigerator. The actual trap is longer and narrower than indicated in the diagram.

thin volume and the area for escape is small compared to the area of the trap. At temperatures below 100 μK the time for an atom to escape can be quite long; the atom is likely to collide before leaving the trap, reducing the efficiency of saddlepoint evaporation.

To reach temperatures lower than 100 μK we use the spin resonance technique of rf evaporation. A radio frequency (rf) field is applied. Resonance occurs when the energy of the rf photons matches the energy splitting between hyperfine states, proportional to the strength of the trapping field. Atoms with energy sufficient to reach the resonance region are transferred to an untrapped hyperfine state and leave the trap. The resonance region is a shell along the length and ends of the trap. The atoms can escape in any direction, restoring the efficiency of evaporation. The introduction of rf evaporation into our cryogenic apparatus allowed us to cool hydrogen into the quantum degenerate regime for the first time [5].

Spectroscopy To study the cold, trapped gas we employ high resolution two-photon spectroscopy of the $1S$-$2S$ transition, taking advantage of the cold-collision frequency shift [6]. The transition is excited at 243 nm by a laser which is stabilized to about 1 kHz. The laser beam passes along the axis of the trap and is retro-reflected by a small mirror at the end of the trapping cell, providing a standing wave. Two-photon excitation in a standing wave leads to two types of absorption: Doppler-sensitive, due to absorption of copropagating photons, and Doppler-free, due to absorption of counterpropagating photons. In the first case the spectrum exhibits a recoil shift and Doppler broadening that can be used to measure the absolute temperature. In the second case, Doppler-free excitation results in a narrow, intense line. The narrow transition allows us to measure the perturbation of the atomic energy levels due to the presence of other atoms. The shift of the $1S$-$2S$ transition frequency is proportional to the local density and is known as the cold-collision frequency shift.

Our detection scheme exploits the long lifetime of the metastable $2S$ state. The transition is driven by a 1.5 ms long laser pulse, and the excited atoms remain in the $2S$ state. They are quenched to the $1S$ state by applying an electric field pulse. The emitted Lyman-α photons are dectected by a microchannel plate. A schematic diagram of the apparatus is shown in Fig. 1.

3 Recent Progress

Our major effort during the past year has been to study the evolution of the hydrogen BEC. In addition, we have made a number of experimental advances: we extended the frequency range and reduced heating in the rf antennas used for evaporation, improved the optical collection efficiency, and largely eliminated stray electric fields in the plastic trapping cell.

3.1 Experimental advances

RF antenna redesign The introduction of rf antennas into the plastic trapping cell made cooling into the degenerate regime possible. However, these coils provided unwanted sources of heat through eddy currents generated in the metallic elements connected to the dilution refrigerator. We desired to reduce this heating and extend the rf range in order to begin rf evaporation at higher frequencies. We moved the rf antennas from the trapping cell to the 4 K vacuum can which surrounds the trapping cell. This involved redesigning the vacuum can to include a plastic segment and winding a superconducting coil of fine wire on the *inside* of this segment. We are now able to use rf-evaporation at frequencies up to 100 MHz with minimal heating of our trapping cell.

The extended rf range makes new experiments possible. For example, 177 MHz is the frequency necessary to drive the $2S$ $F = 1$, $m_F = 1$ to $F = 0$, $m_F = 0$ transition. The $F = 0$, $m_F = 0$ state is anti-trapped, meaning it would be expelled from the trap minimum. By first exciting the atoms to the $2S$ state and then applying a 177 MHz field, we might be able to eject a bright beam of metastable $2S$ atoms. Such a beam could have many interesting applications, possibly including atom lithography.

Improved optical collection Our scheme for detecting metastable $2S$ atoms exploits their long natural lifetime, 122 ms. The $2S$ atoms are excited by a laser pulse and quenched to the $2P$ state by applying an electric field pulse. The emitted Lyman-α photons are detected by a microchannel plate. During the excitation pulse, the 243 nm laser induces fluorescence in the trapping cell which persists for several milliseconds. In the past we used an optical filter to block this fluorescence from the detector. Unfortunately, the same filter also reduces the number of Lyman-α photons detected by a factor of seven. We removed the filter and implemented a switching scheme that energizes the detector only after the fluorescence has died away. We have recently observed signal rates as high as 2×10^5 counts/s.

The increased signal rate permits faster sweeps of the $1S$-$2S$ resonance. In many studies of ultracold hydrogen we rely on the cold-collision frequency shift; a shift of the $1S$-$2S$ frequency proportional to density. Due to dipolar decay, atoms at high densities are quickly lost from the trap, changing the spectrum of the trapped atoms. Any study which makes use of the cold-collision frequency shift should benefit from an increased sweep rate since the lineshape will be changing less between successive sweeps. For example, studies of the formation of a BEC require fine time resolution of the density profile of the condensate.

Reduced stray electric fields In early experiments that employed a cell with metallic walls, we observed the $2S$ lifetime approaching the natural lifetime. However, to achieve BEC we had to switch to a plastic cell which accommodated rf evaporation. In this cell the $2S$ lifetime was never more than a few milliseconds. This shortening was due to stray electric fields resulting from the build up of charges on the insulating cell walls. The $2S$ state lifetime depends strongly on the electric field and even small patches of charge can dramatically shorten it.

To overcome this problem, we coated the inside of the trapping cell with a thin film of copper. This conducting layer prevents the accumulation of charges but allows the penetration of rf-fields used for evaporation. The thickness of the layer is much less than the skin depth of copper for frequencies up to 100 MHz. We have recently observed lifetimes of the $2S$ atoms to be $\sim$100 ms, close to the natural lifetime of 122 ms.

3.2 Study of the evolution of the condensate

In our experiments the size of the condensate is determined by a balance between the rate at which the atoms leave the trap due to two-body spin relaxation (primarily in the condensate) and the rate at which

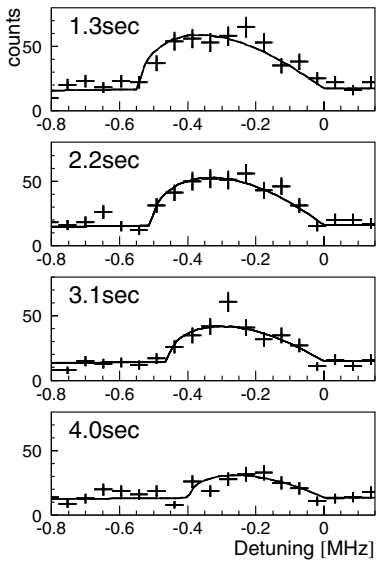

Figure 2: Evolution of a Bose-Einstein condensate of hydrogen: The condensate feature sits on top of the much broader contribution from the normal component in the Doppler-sensitive portion of the two-photon spectrum. Times are measured from the end of forced evaporative cooling.

the condensate is replenished by atoms from the normal (non-condensed) component. The weakness of the interaction between the hydrogen atoms limits how far below the transition temperature the hydrogen can be taken in an equilibrium situation. The small s-wave scattering length, $a = 0.0648$ nm, leads to an elastic scattering rate in the thermal cloud well below that in the alkali metals, thus limiting the evaporative cooling rate. In addition, the weak interaction leads to a high density in the condensate which greatly increases the loss rate. Consequently, the condensate fractions that can be obtained in hydrogen are limited to a few percent. However, the condensate itself can be huge: approximately 10^9 atoms.

Since the condensate contains only a small fraction of the atoms, the normal gas acts as a large reservoir that continually replenishes the condensate as atoms are lost through dipolar relaxation. This replenishment dramatically increases the apparent lifetime of the condensate. We have observed the condensate for more than 10 s. Fig. 2 shows a series of spectra taken at different times after the condensate has formed. The shape of the $1S$-$2S$ spectrum for excitations from the condensate can be explained by assuming that the signal strength at a given detuning is proportional to the number of atoms at the corresponding density. The solid line in Fig. 2 is the spectrum expected from a Thomas-Fermi density distribution in the condensate. The agreement is very good.

We have studied the process of replenishment by obtaining spectra at various hold times after the end of the forced evaporation. The time evolution of the condensate is displayed in Fig. 3, which is a plot of the peak condensate density, n_p, as a function of the hold time (here the sample is held without exposure to the probe laser). The peak condensate density decreases by a factor of two (corresponding to a population decrease of $2^{5/2} \simeq 6$) in 15 s. This should be compared to the characteristic decay time due to dipolar relaxation, $\tau_{dip,c} = 7/(2gn_p)$, where $g = 1.2 \times 10^{-15}$ cm^{-3}/s is the dipolar decay rate constant. For $n_p = 2 \times 10^{15}$ cm^{-3}, $\tau_{dip,c} \simeq 1.5$ s. The 15 s lifetime of the condensate thus indicates feeding of the condensate from the thermal cloud.

The number of atoms fed into the condensate is approximately the number lost during the 15 s shown in Fig. 3. Estimates of the total trap population at $t = 0$ then set an upper limit on the number lost, which scales as $n_p^{7/2}$. This strong dependence provides a useful consistency check on the determination of the peak condensate density from the observed spectral shift. For example, if n_p were actually a factor of two larger

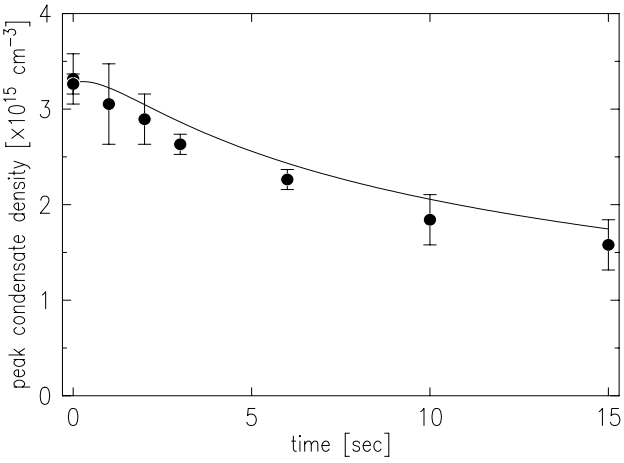

Figure 3: Time evolution of the peak density in the condensate. The solid curve was generated from a model of the loss mechanisms.

than stated here, the entire normal gas would be expended after the 15 s observation.[1] This is clearly not the case since there is still a large condensate present after 15 s.

We have employed a simple model to quantitatively test our understanding of the system. The dynamics is governed by losses due to dipolar relaxation in the condensate and normal gas, and evaporation from the normal gas. Equilibrium between the normal gas and condensate is assumed. The expected behavior is shown by the solid line in Fig. 3. The agreement with experiment indicates a good understanding of the system.

4 Outlook

Our efforts over this past year will enable us to make a more quantitative study of condensate formation dynamics and help us to study highly asymmetric normal gas lineshapes. Furthermore, the large, long-lived $2S$ population that we can create has opened many new opportunities for precision spectroscopy and studies of atomic collisions in hydrogen.

Condensate formation dynamics The kinetics of condensate formation is only partially understood. Formation involves non-equilibrium dynamics of an interacting quantum many-body system. Recent experiments carried out with sodium indicate qualitative agreement between theory and experiment, but the very first stages of formation have not been observed in detail. The slow collision rate in trapped hydrogen gas makes it a good candidate for observing a condensate in its nascent stages.

The formation dynamics of the condensate may be studied by establishing a steady state situation in the magnetic trap at some temperature below the transition temperature, quickly removing some or all of the condensate by rf ejection, then watching the re-establishment of the condensate using $1S$-$2S$ spectroscopy. In this way the precise distribution of densities can be monitored as the condensate grows. Furthermore, atoms may be removed from a specific segment of the density profile, making it possible to observe the re-establishment of the steady state distribution.

[1] In the spectroscopic determination of the condensate density we have used the same constant of proportionality χ between the frequency shift and the density that we found for the normal gas. For excitation out of a Bose condensate, the absence of exchange effects should reduce χ, the frequency shift parameter, by a factor of 2. If this were the case we would obtain maximum condensate densities twice as high and a condensate fraction of 25%, inconsistent with experiment. We do not yet understand the origin of this discrepancy.

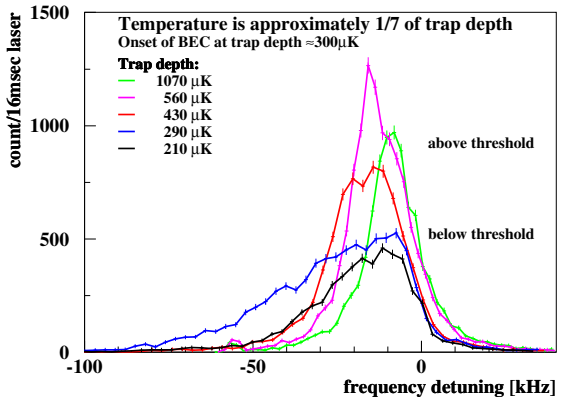

Figure 4: Doppler-free spectrum of the normal fraction immediately after the end of the forced evaporation. The signal in the presence of a condensate (trap depth $\leq 300\ \mu$K) stretches to larger red-shift than expected for a static system in thermal equilibrium.

Asymmetric lineshape In the vicinity of the BEC threshold we have observed unexpectedly broad, asymmetric normal (non-condensed) gas lineshapes. In Fig. 4, we see that much of the signal intensity is red-shifted further than the shift corresponding to the critical density. The volume of the condensate is about 10^{-3} of the volume of the normal cloud, so it is surprising that the condensate appears to affect the spectrum so dramatically. We do not fully understand this lineshape. We plan to carry out a careful study as the transition is approached and crossed.

New opportunities for spectroscopy The observed long lifetime of metastable $2S$ atoms makes the study of other spectroscopic transitions possible. For example, a $2S$ lifetime of ~ 100 ms should make $2S$-nP transitions easy to excite: they are single photon transitions accessible using diode lasers. These transitions would be useful as a diagnostic tool for spectroscopy from the $2S$ state. The most exciting near-term goal for spectroscopy is the study of $2S$-nS two-photon transitions. An accurate measurement of the frequency of these transitions would allow the Lamb shift to be extracted with unprecedented accuracy. These transitions have been studied previously, but our cold trapped hydrogen offers a new arena for spectroscopy, providing important advantages in the extended interaction time.

Publications

Papers

T. J. Greytak, D. Kleppner, D. G. Fried, T. C. Killian, L. Willmann, D. Landhuis, S. C. Moss, "Bose-Einstein condensation in atomic hydrogen", to be published in Physica B.

Lorenz Willmann, "Bose-Einstein Condensation of Atomic Hydrogen", Appl. Phys. B, **69**, 357 (1999).

Thomas C. Killian, "$1S$-$2S$ Spectrum of a Hydrogen Bose-Einstein Condensate", Phys. Rev. A **61**, 033611 (2000).

Theses

Fried, Dale G., *Bose-Einstein Condensation of Atomic Hydrogen*, Ph.D. diss., Department of Physics, MIT, 1999.

Killian, Thomas C., $1S$-$2S$ *Spectroscopy of Trapped Hydrogen: The Cold Collision Frequency Shift and Studies of BEC*, Ph.D. diss., Department of Physics, MIT, 1999.

Vengalattore, Mukund T., *A Frequency Doubling System for Spectroscopy of the Hydrogen* $1S$-$2S$ *Transition*, Senior Thesis, Department of Physics, MIT, 1999.

References

[1] M. Anderson, J. R. Ensher, M. R. Matthews, C. E. Wieman, and E. A. Cornell, Science **269**, 198 (1995).

[2] C. C. Bradley, C. A. Sackett, and R. G. Hulet, Phys. Rev. Lett. **75**, 1687 (1995).

[3] K. B. Davis, M.-O. Mewes, M. R. Andrews, N. J. van Druten, D. S. Durfee, D. M. Kurn, and W. Ketterle, Phys. Rev. Lett. **75**, 3969 (1995).

[4] T. J. Greytak, in *Bose-Einstein Condensation*, edited by A. Griffin, D. W. Snoke, and S. Stringari (Cambridge University Press, Cambridge, England, 1995), a detailed description of trapping and cooling techniques is given in this reference.

[5] D. G. Fried, T. C. Killian, L. Willmann, D. Landhuis, S. C. Moss, D. Kleppner, and T. J. Greytak, Phys. Rev. Lett **81**, 3811 (1998).

[6] T. C. Killian, D. G. Fried, L. Willmann, D. Landhuis, S. C. Moss, D. Kleppner, and T. J. Greytak, Phys. Rev. Lett **81**, 3807 (1998).